Available online at www.sciencedirect.com

ScienceDirect

IFAC PapersOnLine 58-4 (2024) 25–30

Fault Diagnosis using Interval Data-driven LPV Observers and Structural Analysis

Xin Fang,* Joaquim Blesa*, and Vicenç Puig***

* *Institut de Robòtica i Informàtica Industrial, CSIC-UPC, Llorens i Artigas 4-6, 08028 Barcelona, Spain. and Supervision, Safety and Automatic Control Research Center (CS2AC) of the Universitat Politècnica de Catalunya, Rambla Sant Nebridi 22, 08222 Terrassa, Spain*

** *Serra Húnter Fellow, UPC, Automatic Control Department (ESAII), Eduard Maristany 16, 08019 Barcelona, Spain*

Abstract This paper presents a Fault Detection and Isolation (FDI) method that combines Structural Analysis (SA) and machine learning data-driven techniques. The adaptive network fuzzy inference system (ANFIS) is used to obtain a model of the real system to be monitored using historical data from non-faulty scenarios. The structure of the model is given by the SA by means of graphical or textual description of the system. The obtained model is formulated as an observer where unknown but bounded process and sensor noises are considered. Then, LPV observers are used to carry out the fault diagnosis using model residuals. Once observers detect a residual inconsistency, a fault alarm is raised and the fault isolation triggered. Fault isolation is carried out through the transformation of residuals using the Kramer function and the Dempster-Shafer theory. The proposed fault isolation method considers the plausibility of the activation of each residual and the SA information to provide the most probable fault. Finally, a well-known four-tanks system illustrates the performance and results of the proposed method.

1. INTRODUCTION

Fault Diagnosis (FD) is of vital importance in the context of complex industrial systems. The appearance of a fault in an industrial system may result in the interruption or complete paralysis of the whole process, causing huge economical loss. In order to avoid the serious consequence that may influence the performance of these systems, online fault detection and isolation is required. Researchers from various communities, particularly those in the fields of automatic control and artificial intelligence, have been exploring fault diagnosis for an extended period. These two communities consider FD from their own point of view. Consequently, there are two families of FD approaches: the FDI (Fault Detection and Isolation) approaches and the DX (Diagnosis) approaches (Travé-Massuyès, 2014). The FDI approach uses techniques from control theory and statistical decision making. On the other hand, the DX approach uses techniques derived from the fields of logic and computer science. The traditional idea of FD is about using the quantitative model of the system to be monitored, by defining the key indicator named residual, which is the difference between the real output of the system and the prediction output derived from a quantitative model. Ideally, the residual should be zero in the case of the correct system operation, but the presence of modelling uncertainty and external noises make the residual always deviate from zero. In order to distinguish a real fault scenario from residual fluctuations due to modelling error and noises, residual thresholds which include modeling uncertainties can be used to guarantee the correct performance of the fault detection.

In order to cope with this problem, Fang, Puig, and Zhang (2021) introduces a Hybrid FD approach that combines Model-Based and Data-Driven methods. In particular, Structural Analysis (SA) allows to obtain the system model in form of structural graph by-passing the difficulty of obtaining the exact physical model of system, and only requires some essential knowledge about the system functioning. And once the structural model has been achieved and the structural ARRs (Analytical Redundancy Relations) have been obtained, data-driven techniques can be applied to obtain models for ARRs(Goupil, Chanthery, Travé-Massuyès, and Delautier, 2022). Then, the analytical ARRs can be used to develop the system FD. Another FD hybrid method is introduced in (Pulido, Zamarreño, Merino, and Bregon, 2019), this method uses model decomposition techniques to find the ARRs so that a reduced grey-box model can be designed.

Fault isolation aims at identifying the faults affecting the system. Standard fault isolation methods (Blanke, Kinnaert, Lunze, Staroswiecki, and Schröder, 2006) are based on the use of observed binary fault signatures, generated by the detection module, and their relation with all the considered faults and their expected effect in the ARRs. More recent fault isolation approaches are based on the Bayesian reasoning framework as the ones proposed in (Pernestål, Nyberg, and Wahlberg, 2006) and (Fernandez-Canti, Blesa, Tornil-Sin, and Puig, 2015).

Peer review under responsibility of International Federation of Automatic Control.
10.1016/j.ifacol.2024.07.188

This paper presents a hybrid fault diagnosis method that combines structural analysis (SA) and machine learning data-driven algorithms. Given a graphic (or textual) system description and the available inputs/outputs measurements, the structure of analytical redundancy relations (ARRs) between some system inputs and outputs can be determined with the aid of system SA. Then, applying a machine learning data-driven approach (adaptive network fuzzy inference system (ANFIS) (Karaboga and Kaya, 2019)) to historical data in non-faulty scenarios, analytical expressions between inputs and outputs are obtained. Thereby, instead of finding ARRs from physical mathematical model, combining SA and ANFIS using historical data, a set of data-driven ARRs can be obtained and used to implement a diagnosis system. Once the ANFIS model for each ARR has been identified, it is reformulated in a linear parameter varying (LPV) Luenberger observer form. Then, a fault detection scheme based on LPV Interval Observers (combining Kalman filter and pole placement approaches) that take into account unknown but bounded process and sensor noises is developed.

This paper also proposes a new fault diagnosis method that combines the Dempster-Shafer evidence theory (Shafer, 1976) and the Bayesian reasoning to assess the residuals computed considering interval observers in order to determine the most probable fault.

A well-known case study based on a four-tank system is used for illustrative purposes.

The paper has the following structure: Section 2 presents the data-driven model, and it is followed by the Section 3 where interval LPV state estimation for fault detection is developed. In the Section 4, it is presented the fault isolation method based on structural analysis and Dempster-Shafer theory. In Section 5, a case study of four tanks is introduced to show the practical application of the proposed method. Finally, Section 6 draws the conclusions of the present paper.

2. DATA-DRIVEN MODEL

It will be considered a generic system with measured outputs $\boldsymbol{y} \in \Re^{n_y}$ and inputs $\boldsymbol{u} \in \Re^{n_u}$. Then, the behaviour of the system can be described by the following mathematical equations

$$\begin{aligned}\hat{y}_i(k) = & f_i(y_i(k-1),...,y_i(k-n_a),\boldsymbol{y}_{\neg i}(k-1),\\ & ...,\boldsymbol{y}_{\neg i}(k-n_a),\boldsymbol{u}_i(k-1),...,\boldsymbol{u}_i(k-n_a)) \\ & i=1,...,n_y\end{aligned} \tag{1}$$

where

$$\boldsymbol{y}_{\neg i}(k-j) = \boldsymbol{y}(k-j)\backslash y_i(k-j) \quad j=1,...,n_a \tag{2}$$

$$\boldsymbol{u}_i(k-j) = \boldsymbol{u}(k-j) \quad j=1,...,n_a \tag{3}$$

and $f_i()$ is a function that considers the n_a previous values of the measured variables to provide an estimation of the i-th component of $\boldsymbol{y}$ at instant k denoted by $\hat{y}_i(k) \in \Re$.

Defining

$$\boldsymbol{v}_i(k-j) = (\boldsymbol{y}_{\neg i}(k-j) \quad \boldsymbol{u}_i(k-j)) \quad j=1,...,n_a$$

equation (1) can be rewritten as

$$\begin{aligned}\hat{y}_i(k) = & f_i(y_i(k-1),...,y_i(k-n_a),\boldsymbol{v}_i(k-1),...,\boldsymbol{v}_i(k-n_a)) \\ & i=1,...,n_y\end{aligned} \tag{4}$$

In (Fang, Blesa, and Puig, 2023), it was proposed to use an adaptive network-based fuzzy inference system (ANFIS) and calibration data to obtain model (4). In addition, the model was formulated as a LPV state-space (SS) model as follows

$$\begin{aligned}\hat{\boldsymbol{x}}_i(k+1) &= \boldsymbol{A}_i(\boldsymbol{p}_i(k))\hat{\boldsymbol{x}}_i(k) + \boldsymbol{B}_i(\boldsymbol{p}_i(k))\boldsymbol{v}_i(k) \\ \hat{y}_i(k) &= \boldsymbol{C}_i\hat{\boldsymbol{x}}_i(k) + e_i(\boldsymbol{p}_i(k))\end{aligned} \tag{5}$$

3. INTERVAL LPV STATE ESTIMATION AND FAULT DETECTION

Considering that the actual behaviour of the system is affected by process and sensor noises denoted respectively as $\boldsymbol{w}_i(k)$ and $n_i(k)$, model (5) can be expressed as

$$\begin{aligned}\boldsymbol{x}_i(k+1) &= \boldsymbol{A}_i(\boldsymbol{p}_i(k))\boldsymbol{x}_i(k) + \boldsymbol{B}_i(\boldsymbol{p}_i(k))\boldsymbol{v}_i(k) + \boldsymbol{E}_{wi}\boldsymbol{w}_i(k) \\ \boldsymbol{y}_i(k) &= \boldsymbol{C}_i\boldsymbol{x}_i(k) + e_i(\boldsymbol{p}_i(k)) + \boldsymbol{E}_{vi}n_i(k)\end{aligned} \tag{6}$$

In order to obtain a suitable output estimation in the presence of model errors and disturbances, model (5) is formulated as the Luenberger observer

$$\begin{aligned}\hat{\boldsymbol{x}}_i(k+1) &= \boldsymbol{A}_i(\boldsymbol{p}_i(k))\hat{\boldsymbol{x}}_i(k) + \boldsymbol{B}_i(\boldsymbol{p}_i(k))\boldsymbol{v}_i(k) \\ &\quad + \boldsymbol{L}_i(\boldsymbol{p}_i(k))(y_i(k) - \hat{y}_i(k)) \\ \hat{y}_i(k) &= \boldsymbol{C}_i\hat{\boldsymbol{x}}_i(k) + e_i(\boldsymbol{p}_i(k))\end{aligned} \tag{7}$$

As in the case of (5) matrix $\boldsymbol{A}_i$ depends on $\boldsymbol{p}_i(k)$, proportional gain matrix $\boldsymbol{L}_i$ will also depend on $\boldsymbol{p}_i(k)$ and $\boldsymbol{L}_i(\boldsymbol{p}_i(k))$ can be expressed in polytopic form as

$$\boldsymbol{L}_i(\boldsymbol{p}_i(k)) = \sum_{j=1}^{Nv} \mu_i^j(\boldsymbol{p}_i(k))\boldsymbol{L}_i^j \tag{8}$$

where $\boldsymbol{L}_i^j \quad j=1,..,n_v$ are the vertex of $\boldsymbol{L}_i(\boldsymbol{p}_i(k))$.

3.1 *Fault detection strategy*

Considering unknown but bounded process and sensor noises $\boldsymbol{w}_i(k) \in \mathcal{W}$ and $n_i(k) \in \mathcal{V}$ in (6) $\forall k$ where sets $\mathcal{W}$ and $\mathcal{V}$ are zonotopes. A zonotope is composed by a center $\boldsymbol{c} \in \Re^n$ and a generator matrix $\boldsymbol{R} \in \Re^{n\times p}$ and it is defined as a polytopic set which is the linear image of unit hypercube:

$$\langle \boldsymbol{c}, \boldsymbol{R}\rangle = \{\boldsymbol{c} + \boldsymbol{R}\boldsymbol{s}, \|\boldsymbol{s}\|_\infty \le 1\} \tag{9}$$

Then, sets $\mathcal{W}$ and $\mathcal{V}$ can be defined as

$$\begin{aligned}\mathcal{W} &= \langle \boldsymbol{c}_w, \boldsymbol{R}_w\rangle \\ \mathcal{V} &= \langle \boldsymbol{c}_v, \boldsymbol{R}_v\rangle\end{aligned} \tag{10}$$

The IOA (Interval Observer Approach) can be applied to the Luenberger observer defined in (7) by applying zonotope properties and the state estimation can be bounded by the following zonotope

$$\hat{\mathcal{X}}(k) = \langle \boldsymbol{c}_x(k), \boldsymbol{R}_x(k)\rangle \tag{11}$$

where the center $\boldsymbol{c}_x(k)$ and the generator matrix $\boldsymbol{R}_x(k)$ of the zonotope can be recursively computed using

$$\begin{aligned}&\boldsymbol{c}_x(k+1) = (\boldsymbol{A}_i(\boldsymbol{p}_i(k)) - \boldsymbol{L}_i(\boldsymbol{p}_i(k))\boldsymbol{C}_i)\, \boldsymbol{c}_x(k) \\ &+\boldsymbol{B}_i(\boldsymbol{p}_i(k))\boldsymbol{v}_i(k) + \boldsymbol{L}_i(\boldsymbol{p}_i(k))y_i(k) \\ &\boldsymbol{R}_x(k+1) = (((\boldsymbol{A}_i(\boldsymbol{p}_i(k)) - \boldsymbol{L}_i(\boldsymbol{p}_i(k))\boldsymbol{C}_i)\, \boldsymbol{R}_x(k) \\ &\quad \boldsymbol{E}_{wi} \quad -\boldsymbol{L}_i(\boldsymbol{p}_i(k))\boldsymbol{E}_{vi})\end{aligned} \tag{12}$$

In the same way, output prediction calculation $\hat{y}_i(k)$ can be also bounded by a zonotope

$$\hat{y}_i(k) \in \langle c_y(k), \boldsymbol{R}_y(k)\rangle \tag{13}$$

whose center and matrix generator can be computed as

$$\begin{aligned}c_y(k) &= \boldsymbol{C}_i\boldsymbol{c}_x(k) \\ \boldsymbol{R}_y(k) &= [\boldsymbol{C}_i\boldsymbol{R}_y(k) \quad \boldsymbol{E}_{vi}]\end{aligned} \tag{14}$$

The consistency of actual output $y_i(k)$ and model (7) can be assessed by means the residual defined as

$$r_i(k) = y_i(k) - c_y(k) \tag{15}$$

Then, the fault detection considering the IOA can be carried out by means of checking

$$\begin{cases} r_i(k) \notin \langle 0, \boldsymbol{R}_y(k)\rangle \Rightarrow \text{ Fault} \\ \text{Otherwise} \Rightarrow \text{ No Fault} \end{cases} \tag{16}$$

where the zonotope

$$\langle 0, \boldsymbol{R}_y(k)\rangle \tag{17}$$

contains all the possible fault free residuals (consistent with the process and sensor noises).

In (Fang et al., 2023), it was proposed to use two different IOAs to carry out the fault detection: Kalman filter and Pole placement observers. As in a fault free scenario in the presence only of modelling errors and sensor noises, the Kalman filter IOA should provide the optimal estimation, it is expected that the fault detection test based on this filter will be the first that will detect a inconsistency when a fault appears in the system. However, once the fault is present in the system, Kalman observer will lose the optimality and the Pole placement observer, designed to minimise the fault following effect, is expected to have a better performance to maintain the fault detection signal active after the fault appearance.

Once observer gains $\boldsymbol{L}_i^j \quad j = 1,..,N_v$ are computed following the Kalman filter and Pole placement approaches, fault detection test defined in equation (16) can be applied in parallel for the Kalman filter and Pole placement approach. i.e. two different detection tests will be running at the same time. When one of the two fault detection tests will find and inconsistency, it will be consider that a fault is present in the system.

4. STRUCTURAL ANALYSIS AND FAULT ISOLATION

Based on knowledge of the system obtained from its graphic or textual description, analysing the different system components, the structural model can be obtained, which is a set of constraints between system inputs and outputs. The structural model will be the starting point for structural analysis.

The basic tool for the structural analysis is the concept of matching in bipartite graphs. In simple terms, a matching is a causal assignment which associates with every unknown system variable a constraint that can be used to determine the variable (Blanke et al., 2006). In most of the cases, the matching is not unique, so that variables which can be matched in several ways can be determined in different (redundant) ways. The last situation provides a means for fault detection and for reconfiguration.

Using matching process approach described in (Blanke et al., 2006), a set of n_y ARRs as the ones defined in (1) but that can have less components in $\boldsymbol{y}_{\neg i}(k-j)$ and in $\boldsymbol{u}_i(k-j)$ defined in (2) and (3) can be obtained. So, the process of model calibration considering the n_y ARRs obtained in the structural analysis will involve less computational cost than considering that all input/output variables are related, as considered in $\boldsymbol{y}_{\neg i}(k-j)$ and in $\boldsymbol{u}_i(k-j)$. In addition, the structural information can be used for fault isolation purposes.

Once a fault has been detected, The fault isolation can be performed by considering the theoretical *Fault Signature Matrix* (FSM), denoted as $\boldsymbol{FSM}$. The elements of matrix $\boldsymbol{FSM}$: FSM_{ij} $i = 1, ..., n_y$ and $j = 1, ..., n_f$, where n_f number of different considered faults, are binary values and indicate the theoretical incidence of the n_f faults on the n_y residuals. i.e. FSM_{ij} will be equal to 1 if the fault f_j affects the computation of the residual r_i and 0 otherwise. This binary information is provided by the structural analysis of the system.

The columns of the $\boldsymbol{FSM}$ are known as *theoretical fault signatures* and indicate which residuals are affected by a given fault f_j. Two faults i and j will be *isolable* if columns i and j of $\boldsymbol{FSM}$ are different while the two faults will be indistinguishable faults if columns i and j of $\boldsymbol{FSM}$ are identical. The fault isolation consist in checking the matching between the different *theoretical fault signatures* and a *diagnostic signal* $\phi^T = (\phi_1(k), \cdots, \phi_{ny}(k))$

Diagnostic signal can be a binary vector also known as observed fault signature whose components $\phi_i(k)$ $i = 1, ..., n_y$ indicate if residual $r_i(k)$ is consistent with historical fault-free data ($\phi_i(k) = 0$) or not ($\phi_i(k) = 1$).

However, the fault diagnostic signal (or fault signal) for each residual can be computed in a non-binary way in order to obtain a more accurate fault diagnosis and avoid the noise chattering effect. As in (Puig and Blesa, 2013), where fault signals were calculated using the Kramer function (Petti, Klein, and Dhurjati, 1990)

$$\phi_i(k) = \begin{cases} \frac{(r_i(k)/r_{i,\max}(k))^4}{1+(r_i(k)/r_{i,\max}(k))^4} & if \quad r_i(k) \geq 0 \\ \\ \frac{(r_i(k)/r_{i,\min}(k))^4}{1+(r_i(k)/r_{i,\min}(k))^4} & if \quad r_i(k) < 0 \end{cases} \tag{18}$$

where $r_{i,\min}(k)$ and $r_{i,\max}(k)$ are minimum and maximum values comptuted by IOA observers obtained by means applying the interval hull to the residual zonotope (17). The purpose of $\phi_i(k)$ is to normalize the residuals in a range $[0, 1)$, i.e. $\phi_i(k) \in [0, 1)$ introducing a grade in the residual evaluation: $\phi_i(k) = 0$ perfect case, $\phi_i(k) = 0.5$ residual violated, $\phi_i(k) \approx 1$ residual severely violated and all of the intermediate cases.

In addition, a slide window with width T_w can be defined in order to find the maximum values of $\phi_i(k)$ defined in (18) inside the window as follows

$$\phi_{i,\max}(k) = \max_{k \in [k, k-T_w]} (|\phi_i(k)|) \tag{19}$$

In this way, using $\phi_{\max}^T = (\phi_{1,\max}(k), \cdots, \phi_{nr,\max}(k))$ in the fault isolation process the effect of the changes in the residual values due to noise and fault-following effects are minimized because only the peaks of fault signal are stored.

4.1 Dempster-Shafer evidence theory

The Dempster-Shafer Theory (DST) (Shafer, 1976) is the mathematical framework in order to handle uncertainty and make decisions in presence of evidence from different sources or same source at different time instants. These evidences can be incomplete or conflicting.

In a given situation, considering all possible hypotheses which are mutually exclusive and exhaustive, this global set is called Frame of Discernment, denoted as θ. The DST defines three key parameters for considered situation: Mass Function (m), Plausibility Function (Pl), Believe Function (Bel). Mass Function (m) is pre-assigned to every possible subset of the frame of discernment based on available information, e.g. the expert knowledge. $m(\mathcal{A})$ represents the degree of believe or evidence in favor of hypothesis $\mathcal{A}$. The mass function is defined over the power set of θ denoted as 2^θ. The plausibility function defines the degree to which a hypothesis is plausible with evidence. It is calculated as the sum of all subsets of θ which include the hypothesis, i.e. for the hypothesis $\mathcal{A}$, $Pl(\mathcal{A}) = \sum_{\mathcal{B}_i|\mathcal{A}\in\mathcal{B}_i} m(\mathcal{B}_i)$. The belief function measures the degree of belief for a hypothesis, it can be defined as the sum of subsets of θ that only contain the the hypothesis $\mathcal{A}$, $Bel(\mathcal{A}) = \sum m_i(\mathcal{A})$.

Considering FSM $\in \{0,1\}^{n_y\times n_f}$ obtained from structural analysis and the observed fault signal $\phi_{\max}$, the main challenge of carrying out a fault diagnosis procedure is to cope with the effect of the model uncertainty of the IOA, i.e. the thickness of residual bounds $r_{i,\min}(k)$ and $r_{i,\max}(k)$ that can mask the effect of faults in residuals. The probability mass of faults $f_j \quad j = 1,...,n_f$ can be computed as

$$m(f_j) = \frac{m(f_j)}{\alpha} \quad j = 1,...,n_f \tag{20}$$

where

$$m(f_j) = \prod_{i=1}^{n_r} P(\phi_{i,\max}|f_j) \tag{21}$$

with

$$P(\phi_{i,\max}|f_j) = \begin{cases} \phi_{i,\max} & \text{if} \quad FSM_{j,i} = 1 \\ 1-\phi_{i,\max} & \text{if} \quad FSM_{j,i} = 0 \end{cases} \tag{22}$$

and α is a normalization constant.

On the other hand, other hypotheses as that only one of the n_y residuals has been activated can be defined. The probability mass of this hypothesis for every residual r_i $i = 1,...,n_y$ can be computed as

$$m(r_i) = \frac{m(r_i)}{\alpha} \quad i = 1,...,n_y \tag{23}$$

with

$$m(r_i) = \phi_{i,\max} \prod_{j\in\{1,...,n_y\}\setminus i}^{n_y} (1-\phi_{j,\max}) \tag{24}$$

Then, normalization constant α can be computed as

$$\alpha = \sum_{j=1}^{n_f} m(f_j) + \sum_{i=1}^{n_y} m(r_i) \tag{25}$$

Faults beliefs are directly obtained from faults probability mass by

$$Bel(f_j) = m(f_j) \quad j = 1,...,n_f \tag{26}$$

But in the case of fault plausabilities, mass residual hypothesis (23) that fit with the theoretical $\boldsymbol{FSM}$ have to be considered

$$pl(f_j) = m(f_j) + \sum_{i=1}^{n_y} m(r_i) FSM_{j,i} \tag{27}$$

Finally, given a fault signal $\phi_{\max}$, the fault likelihoods can be obtained as

$$p(\phi_{\max}|f_j) = \frac{pl(f_j)}{\sum_{l=1}^{n_f} pl(f_l)} \tag{28}$$

4.2 Computation of the posterior probabilities

Given the $\boldsymbol{FSM}$ and the fault signals at time instant k: $\phi^T_{\max}(k) = (\phi_{1,\max}(k), \cdots, \phi_{ny,\max}(k))$, the isolation of a particular fault from the $\boldsymbol{FSM}$ can be performed by means of the computation of each fault posterior probability by applying the Bayes rule:

$$p(f_j|\phi_{\max}(k)) = \frac{p(\phi_{\max}(k)|f_j)p(f_j)}{\sum_{l=1}^{n_f} p(\phi_{\max}(k)|f_l)p(f_l)} \tag{29}$$

where $p(f_j)$ is the prior probability assigned to fault f_j, $p(f_j|\phi_{\max}(k))$ is the posterior probability assigned to fault f_j, and $p(\phi_{\max}(k)|f_j)p(f_j)$ is the likelihood that the fault f_j is behind the observed fault signal $\phi_{\max}(k)$ computed by (28). Finally, posterior probabilities (29) can be computed recursively as long as new measurements become available, since the posterior probabilities (29) can be used as prior probabilities in successive iterations, i.e. $p(f_j) = p(f_j|\phi_{\max}(k-1))$.

5. APPLICATION EXAMPLE: FOUR-TANKS SYSTEM

The considered system in this section is the quadruple-tank (Johansson, 2000), used in (Blesa, Puig, and Saludes, 2012) with the aim of performing fault diagnosis. The inputs and outputs of the system are related by the following model derived from physical principles

$$\begin{aligned} &y_1(k) = y_1(k-1) - \tfrac{a_1}{A_1}\sqrt{2gy_1(k-1)} + \tfrac{a_3}{A_1}\sqrt{2gy_3(k-1)} \\ &+\tfrac{\gamma_1 k_1}{A_1}u_1(k-1) \\ &y_2(k) = y_2(k-1) - \tfrac{a_2}{A_2}\sqrt{2gy_2(k-1)} + \tfrac{a_4}{A_2}\sqrt{2gy_4(k-1)} \\ &+\tfrac{\gamma_2 k_2}{A_2}u_2(k-1) \\ &y_3(k) = y_3(k-1) - \tfrac{a_3}{A_3}\sqrt{2gy_3(k-1)} + \tfrac{(1-\gamma_2)k_2}{A_4}u_2(k-1) \\ &y_4(k) = y_4(k-1) - \tfrac{a_4}{A_4}\sqrt{2gy_4(k-1)} + \tfrac{(1-\gamma_1)k_1}{A_4}u_1(k-1) \end{aligned} \tag{30}$$

where the inputs u_1 and u_2 are voltages of two pumps and the outputs y_1, y_2, y_3 and y_4 are the levels of four tanks.

Considering the output estimation model (1), the a first order model f_i is considered and only information of input and output are used. Thus, the model (4) in this particular case with four outputs and two inputs can be expressed as follows:

$$\hat{y}_i(k) = f_i(y_i(k-1), \boldsymbol{v}_i(k-1)) \quad i = 1,...,4 \tag{31}$$

where

$$\boldsymbol{v}_i(k-1) = (\boldsymbol{y}_{\neg i}(k-1) \quad u_1(k-1) \quad u_2(k-1))\; i = 1,...,4 \tag{32}$$

However, applying structural analysis with the elementary relations of the different components of the system, as proposed in Fang et al. (2023), the following set of of models are obtained

$$\begin{aligned} \hat{y}_1(k) &= f_1(y_1(k-1), y_3(k-1), u_1(k-1)) \\ \hat{y}_2(k) &= f_2(y_2(k-1), y_4(k-1), u_1(k-1)) \\ \hat{y}_3(k) &= f_3(y_3(k-1), u_2(k-1)) \\ \hat{y}_4(k) &= f_4(y_4(k-1), u_1(k-1)) \end{aligned} \tag{33}$$

With the aid of structural analysis, the number of variables implicated in equations is reduced remarkably comparing to (31). In addition, structural analysis can also be used to study the effect of the faults in residuals obtained comparing output measurements and estimations (31). In particular, considering sensors faults f_{y_1}, f_{y_2}, f_{y_3} ,f_{y_4} and actuator faults f_{k_1}, f_{k_2}. This dependence can be summarized in the FSM of Table 1. Afterwards, the ANFIS

Table 1. Theoretical FSM

	f_{y_1}	f_{y_2}	f_{y_3}	f_{y_4}	f_{k_1}	f_{k_2}
r_1	1	0	1	0	1	0
r_2	0	1	0	1	0	1
r_3	0	0	1	0	0	1
r_4	0	0	0	1	1	0

data-driven method is applied using some available fault free historical data, by considering the minimal number of branches in fuzzification layer ($m_f = 2$) and input variable number ($n_u = 2$), the following LPV-IO model is obtained

$$\hat{y}_3(k) = -\left(\sum_{j=1}^{4}(\mu_3^j(\boldsymbol{p}_3(k))a_3^j\right) y_3(k-1) + \left(\sum_{j=1}^{4}(\mu_3^j(\boldsymbol{p}_3(k))b_3^j)\right) u_2(k-1) + \left(\sum_{j=1}^{4}(\mu_3^j(\boldsymbol{p}_3(k))e_3^j\right) \quad (34)$$

where

$$\boldsymbol{p}_3(k) = (y_3(k-1) \quad u_2(k-1)). \quad (35)$$

Thereby, the LPV-IO form shown before can be rewritten in state-space form as follows

$$\begin{aligned} \hat{\boldsymbol{x}}_3(k+1) &= \boldsymbol{A}_3(\boldsymbol{p}_3(k))\hat{\boldsymbol{x}}_3(k) + \boldsymbol{B}_3(\boldsymbol{p}_3(k))\boldsymbol{v}_3(k) \\ \hat{y}_3(k) &= \boldsymbol{C}_3\hat{\boldsymbol{x}}_3(k) + e_3(\boldsymbol{p}_3(k)) \end{aligned} \quad (36)$$

where

$$\begin{aligned} \boldsymbol{A}_3(\boldsymbol{p}_3(k)) &= -a_{3,1}(\boldsymbol{p}_3(k)) \\ \boldsymbol{B}_3(\boldsymbol{p}_3(k)) &= b_{3,1}(\boldsymbol{p}_3(k)) \\ \boldsymbol{C}_3 &= 1 \\ \boldsymbol{x}_3(k) &= y_3(k) \end{aligned} \quad (37)$$

As mentioned in Sections 3.1 and 3.2, two observers (Kalman filter and Pole placement) have been considered. The thresholds $r_{i,\min}(k)$ and $r_{i,\max}(k)$ are computed with the IOA. Analogoulsy, the rest three LPV-IO state space models ($\hat{y}_1(k)$. $\hat{y}_2(k)$ and $\hat{y}_4(k)$) can be obtained in the same way. Figure 1 shows the evolution of the residual values and bounds using Kalman and Pole Placement observers in a fault free scenario. As it can be seen, the thickness of residual thresholds is wider in the case of the pole placement observers because they are tuned to mitigate the fault following effect using slow poles.

Figure 2 depicts the evolution of residual values and bounds using the two IOA in a sensor y_4 fault scenario (f_{y4}=4cm) at time instant 200s. As it can be seen, in both approaches residuals r_2 and r_4 violate their residual bounds. That is consistent with the the FSM of Table 1 (the column f_{y4} whose components corresponding to residuals r_2 and r_4 are the only ones that are $'1'$). It can also be observed that, once the fault is present in the system the Kalman filter approach presents an inconvenient feature the"fault following effect", which shows the tendency of the estimation model to follow the faulty output leading

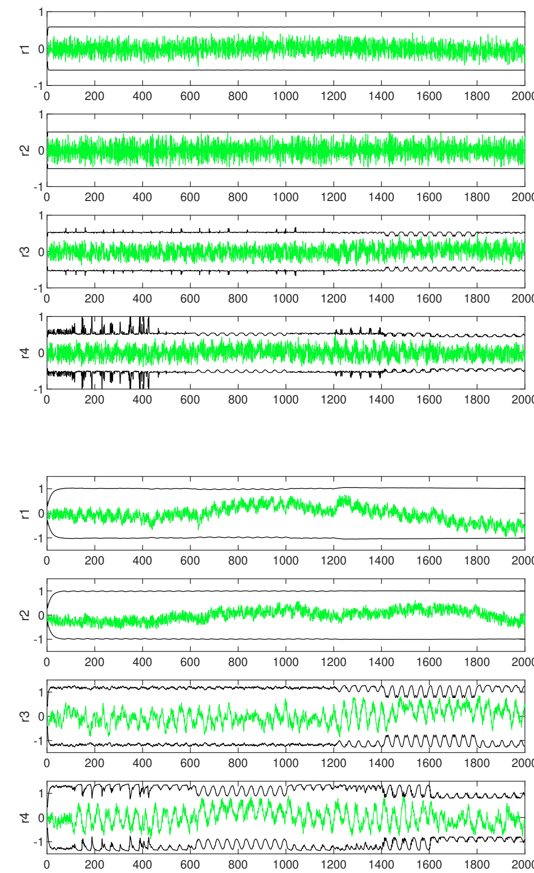

Figure 1. Evolution of residual values (green) and bounds (black) using Kalman (Up) and Pole Placement (Down) observers in a fault free scenario

to a non-persistent activation of the inconsistency in residuals. The pole placement observer is much less sensitive to this undesired effect, as previously discussed. In order to better combine the performance in a fault free scenario and after a fault is present in the system of Kalman filter and Pole Placement approaches respectively, the Kalman filter is used to detect faults. But, once the fault is detected in the system, pole placement observer residuals are used to analyze the evolution of the fault in the system.

Finally, Figure 3 shows the results of the fault isolation method proposed in this paper in the sensor fault scenario f_{y_4} described before. This figure presents the posterior probabilities (29) obtained by the fault isolation method for every fault considered in Table 1. i.e. f_{y_1}, f_{y_2}, f_{y_3}, f_{y_4}, f_{k_1} and f_{k_2} denoted as F_1, F_2, F_3, F_4, F_5 and F_6 respectively in the subplots of the figure. As it can be seen, the posterior probabilities converge quickly to the correct isolation of fault f_{y_4} (i.e F_4).

6. CONCLUSION

This paper has introduced a method combining SA and data-driven techniques in order to avoid the difficulty of obtaining a physical model of a real system for FDI purposes. The proposed method integrates IOA to consider different uncertainties of the real system in order to develop a more accurate fault detection. In addition,

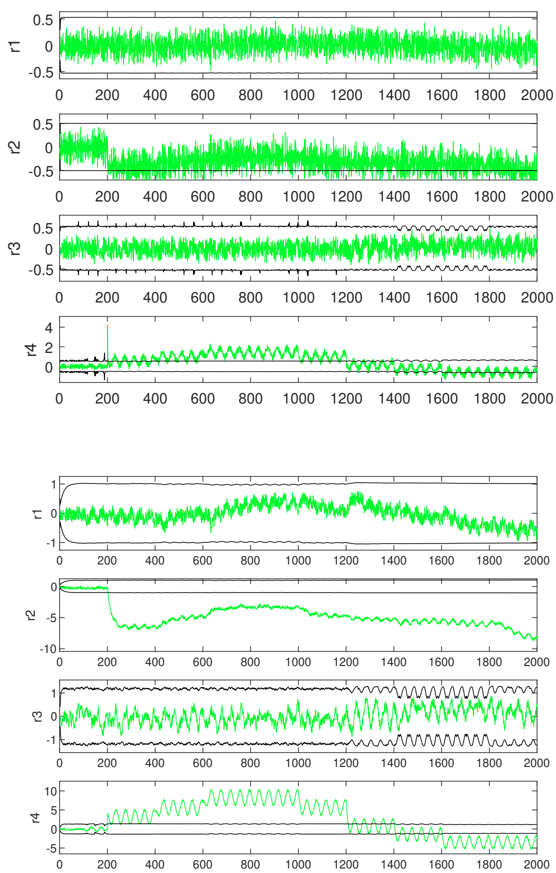

Figure 2. Evolution of residual values (green) and thresholds (black) using Kalman (Up) and Pole Placement (Down) observers in a sensor fault scenario f_{y_4}

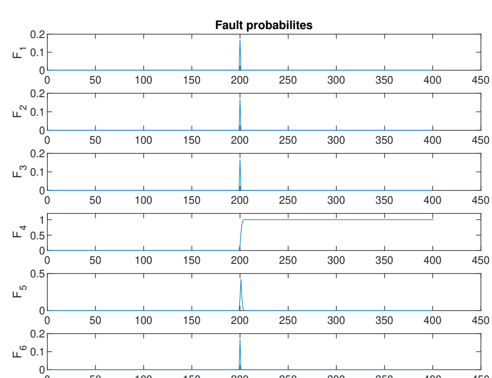

Figure 3. Fault isolation in the sensor fault scenario f_{y_4}

the Dempster-Shafer Theory has been proposed to implement the fault isolation by means the computation of the plausibility of each residual. Finally, the application example based on four-tanks system has illustrated the performance of the proposed method.

ACKNOWLEDGEMENTS

This work has been co-financed by the Spanish Research Agency (AEI) through the projects SaCoAV (ref. MINECO PID2020-114244RB-I00) and L-BEST (PID2020-115905RB-C21).

REFERENCES

Blanke, M., Kinnaert, M., Lunze, J., Staroswiecki, M., and Schröder, J. (2006). *Diagnosis and fault-tolerant control*, volume 2. Springer.

Blesa, J., Puig, V., and Saludes, J. (2012). Robust identification and fault diagnosis based on uncertain multiple input–multiple output linear parameter varying parity equations and zonotopes. *Journal of Process Control*, 22(10), 1890–1912.

Fang, X., Blesa, J., and Puig, V. (2023). Fault detection using data-driven lpv state estimation based on structural analysis and anfis. In *2023 European Control Conference (ECC)*, 1–6. IEEE.

Fang, X., Puig, V., and Zhang, S. (2021). Fault diagnosis and prognosis using a hybrid approach combining structural analysis and data-driven techniques. In *2021 5th International Conference on Control and Fault-Tolerant Systems (SysTol)*, 145–150. IEEE.

Fernandez-Canti, R.M., Blesa, J., Tornil-Sin, S., and Puig, V. (2015). Fault detection and isolation for a wind turbine benchmark using a mixed bayesian/set-membership approach. *Annual Reviews in Control*, 40, 59–69.

Goupil, L., Chanthery, E., Travé-Massuyès, L., and Delautier, S. (2022). A survey on diagnosis methods combining dynamic systems structural analysis and machine learning. In *33rd International Workshop on Principle of Diagnosis–DX 2022*.

Johansson, K.H. (2000). The quadruple-tank process: A multivariable laboratory process with an adjustable zero. *IEEE Transactions on control systems technology*, 8(3), 456–465.

Karaboga, D. and Kaya, E. (2019). Adaptive network based fuzzy inference system (anfis) training approaches: a comprehensive survey. *Artificial Intelligence Review*, 52(4), 2263–2293.

Pernestål, A., Nyberg, M., and Wahlberg, B. (2006). A bayesian approach to fault isolation-structure estimation and inference. *IFAC Proceedings Volumes*, 39(13), 450–455.

Petti, T.F., Klein, J., and Dhurjati, P.S. (1990). Diagnostic model processor: using deep knowledge for process fault diagnosis. *AIChE Journal*, 36(4), 565–575.

Puig, V. and Blesa, J. (2013). Limnimeter and rain gauge fdi in sewer networks using an interval parity equations based detection approach and an enhanced isolation scheme. *Control Engineering Practice*, 21(2), 146–170.

Pulido, B., Zamarreño, J.M., Merino, A., and Bregon, A. (2019). State space neural networks and model-decomposition methods for fault diagnosis of complex industrial systems. *Engineering Applications of Artificial Intelligence*, 79, 67–86.

Shafer, G. (1976). *A mathematical theory of evidence*, volume 42. Princeton university press.

Travé-Massuyès, L. (2014). Bridging control and artificial intelligence theories for diagnosis: A survey. *Engineering Applications of Artificial Intelligence*, 27, 1–16.